Natural Product Research

Formerly Natural Product Letters

ISSN: 1478-6419 (Print) 1478-6427 (Online) Journal homepage: https://www.tandfonline.com/loi/gnpl20

Isolation, Synthesis And Structure Determination Of Cannabidiol Derivatives And Their Cytotoxic Activities

Yedukondalu Nalli, Suraya Jan, Gianluigi Lauro, Javeed Ur Rasool, Waseem I. Lone, Aminur R. Sarkar, Junaid Banday, Giuseppe Bifulco, Hartmut Laatsch, Sajad H. Syed & Asif Ali

To cite this article: Yedukondalu Nalli, Suraya Jan, Gianluigi Lauro, Javeed Ur Rasool, Waseem I. Lone, Aminur R. Sarkar, Junaid Banday, Giuseppe Bifulco, Hartmut Laatsch, Sajad H. Syed & Asif Ali (2019): Isolation, Synthesis And Structure Determination Of Cannabidiol Derivatives And Their Cytotoxic Activities, Natural Product Research, DOI: 10.1080/14786419.2019.1638381

To link to this article: https://doi.org/10.1080/14786419.2019.1638381

NATURAL PRODUCT RESEARCH
https://doi.org/10.1080/14786419.2019.1638381

Taylor & Francis
Taylor & Francis Group

Isolation, Synthesis And Structure Determination Of Cannabidiol Derivatives And Their Cytotoxic Activities

Yedukondalu Nalli[a,b], Suraya Jan[b,c], Gianluigi Lauro[d], Javeed Ur Rasool[a,b], Waseem I. Lone[a,b], Aminur R. Sarkar[a], Junaid Banday[a], Giuseppe Bifulco[d], Hartmut Laatsch[e], Sajad H. Syed[b,c] and Asif Ali[a,b]

[a]Natural Product Chemistry Division, CSIR-Indian Institute of Integrative Medicine, Canal Road, Jammu-Tawi, J&K, 180001, India; [b]Academy of Scientific and Innovative Research, New Delhi, India; [c]Pharmacology Division, CSIR-Indian Institute of Integrative Medicine, Canal Road, Jammu, Sanatnagar Srinagar, 180001, India and 190005; [d]Department of Pharmacy, University of Salerno, Via Giovanni Paolo II 132, Fisciano, 84084, Italy; [e]Institute of Organic and Biomolecular Chemistry, University of Göttingen, Tammannstr. 2, Göttingen, D-37077, Germany

ABSTRACT

In a continuing effort to explore the structural diversity and pharmacological activities of natural products based scaffolds, herein, we report the isolation, synthesis, and structure determination of cannabidiol and its derivatives along with their cytotoxic activities. Treatment of cannabidiol (**1**) with acid catalyst $POCl_3$ afforded a new derivative **6** along with six known molecules **2** – **5**, **7** and, **8**. The structure of **6** was elucidated by extensive spectroscopic analyses and DFT calculations of the NMR and ECD data. All the compounds (**2** – **8**) were evaluated for their cytotoxic potential against a panel of eight cancer cell lines. Compounds **4**, **5**, **7**, and **8** showed pronounced *in vitro* cytotoxic activity with IC_{50} values ranging from 5.6 to 60 μM. Out of the active molecules, compounds **4**, and **7** were found to be comparable to that of the parent molecule **1** on the inhibition of almost all the tested cancer cell lines.

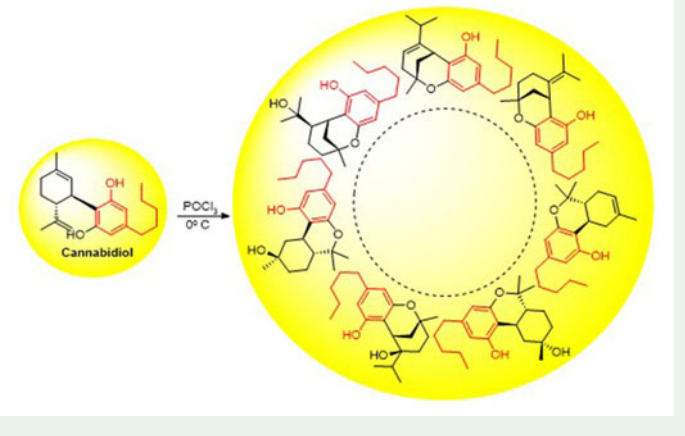

ARTICLE HISTORY
Received 16 May 2018
Accepted 27 June 2019

KEYWORDS
Cannabis sativa L.; Cannabinoids; Cannabidiol; Divergent synthesis; Cytotoxic activities

CONTACT Asif Ali asifali@iiim.ac.in

Supplemental data for this article can be accessed at https://doi.org/10.1080/14786419.2019.1638381.

1. Introduction

Cannabis sativa L. (CS) has been a part of Indian medicinal and spiritual culture since as early as 2000 BC (Singh 2016). CS is a prolific producer of structurally diverse phytocannabinoids including cannabigerol (CBG), cannabidiol (CBD), tetrahydrocannabinol (Δ^9-THC), and cannabichromene (CBC) and their corresponding acidic versions as major constituents (Radwan et al. 2015). The structural diversity of cannabinoids of CS has partially attributed to the non-enzymatic transformations of these major constituents induced by heat, light, pH and atmospheric oxygen (Hanus et al. 2016). In recent years, cannabinoids and their derivatives have drawn renewed attention due to their diverse pharmacological activities such as cell growth inhibition, anti-inflammatory effects, tumour regression (Di Marzo and Piscitelli 2015, Luciano et al. 2011, Nalli et al. 2018). Furthermore, the U.S. Food and Drug Administration (FDA) have approved three cannabinoid-based drugs (Marinol, Syndros, Cesamet) for the treatment of AIDS wasting syndrome, epilepsy, neuropathic pain, spasticity associated with multiple sclerosis, and chemotherapy-induced nausea (Seely et al. 2011). In order to explore the structural diversity and pharmacological activities of cannabinboid based scaffolds, a small compound library was synthesize based on the non-psychoactive cannabinoid CBD by using $POCl_3$ as an acid catalyst (Nalli et al. 2016, Nalli et al. 2017). Herein, we report the isolation, synthesis, structural determination of CBD analogs, and their cytotoxic potential against a panel of eight human cancer cell lines.

2. Results and discussion

Compound **1** was isolated as a major constituent from the leaves of *Cannabis sativa* L., collected from the Botanical garden of the CSIR-Indian Institute of Integrative Medicine, Jammu (India). The plant was identified by a taxonomist Dr. Sumeet Gairola, and a voucher specimen (IIIM 23453) was deposited at the Herbarium of the IIIM, Jammu (India). During our efforts on semi-synthetic modifications of cannabidiol (**1**), was reacted with acid catalyst $POCl_3$ at 0 °C for five minutes, the formation of seven major products were observed. All these products (**2** – **8**) were isolated by extensive column chromatography over sephadex LH-20 followed by semi-preparative HPLC using RP-C8 column affording seven compounds (Figure 1). The structures of compounds **2** – **8** were characterized by HR-ESI-MS, and 1 D- and 2 D-NMR spectroscopic studies disclosed compound **6** as a new structure. Among known compounds, **2** (Δ^4-isotetrahydrocannabinol) (Crombie et al. 1988), **3** (**$\Delta^{4(8)}$**-isotetrahydrocannabinol) (Crombie, Crombie, Jamieson and Palmer 1988), **4** (Δ^8-tetrahydrocannabinol) (Cheng et al. 2013), and **5** (9α-hydroxyhexahydrocannabinol) (Cheng, Xie, Chen, Wang and Zhou 2013) were known in the literature as secondary metabolites of *Cannabis sativa* L.; on the other hand, **7** (9β-hydroxyhexahydrocannabinol) (Cheng, Xie, Chen, Wang and Zhou 2013), and **8** (8-hydroxy-isohexahydrocannabinol) (Turner et al. 1981) have been reported as synthetic compounds. The structure of compound **6** was determined on the basis of detailed analysis of MS and NMR spectral data. Compound **6** was obtained as brown, viscous oil. The molecular formula, $C_{21}H_{32}O_3$, was established by the presence of $[M+H]^+$ ion at *m/z* 333.2421 in the HR-ESI-MS spectrum, indicating

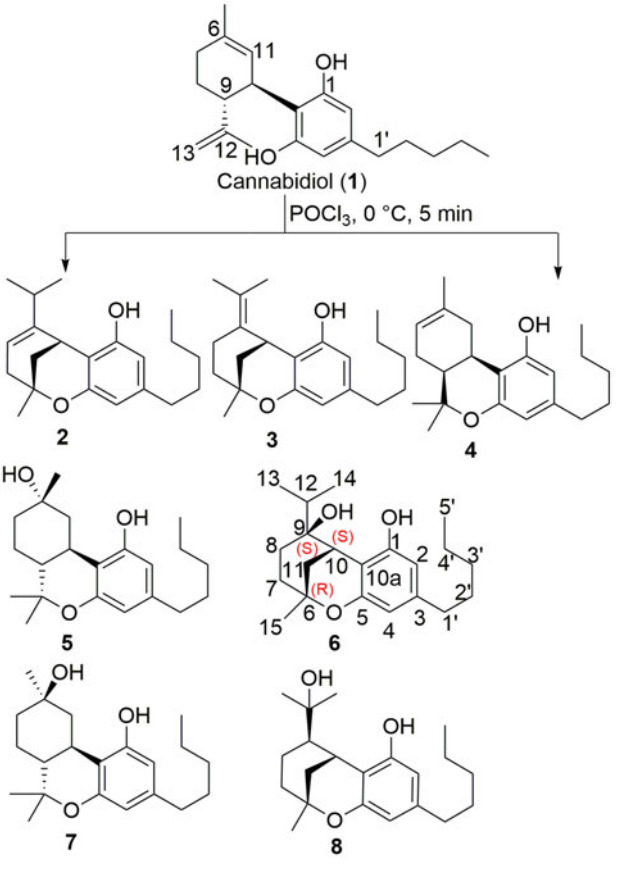

Figure 1. Reagents and conditions: CBD (1 g, 3.01 mmol), $POCl_3$ (3 mL, 31.1 mmol), at 0 °C, 5 min.

six indices of hydrogen deficiency. A close inspection of the ^{1}H-, ^{13}C-, and HSQC-NMR spectra of **6** revealed the presence of four sp^2 quaternary carbons (C-1, C-3, C-5, and C-10a), two aromatic methines (C-2 and C-4), two sp^3 oxygenated quaternary carbons (C-6 and C-9), two sp^3 methines (C-10 and C-12), seven sp^3methylenes (C-1′, C-2′, C-3′, C-4′, C-7, C-8, and C-11), and four methyl carbons (C-5′, C-13, C-14, and C-15) (Figure S10). The ^{1}H-^{1}H COSY analysis of **6** led to four partial structural units: H-7 (δ_H 1.96 – 1. 78) ⟺ H-8 (δ_H 1.51, 1.34); H-13 (δ_H 1.11) ⟺ H-12 (δ_H 1.69) ⟺ H-14 (δ_H 0.78); H-10 (δ_H 3.26) ⟺ H-11 (δ_H 2.42 – 2.36); and H-1′ (δ_H 2.47 – 2.42) ⟺ H-2′ (δ_H 1. 31) ⟺ H-3′ (δ_H 1.58) ⟺ H-4′ (δ_H 1.33) ⟺ H-5′ (δ_H 0.89) as shown by bold-faced lines in Figure S10. Above spin systems were connected to each other on the basis of HMBC correlations. The HMBC spectrum showed key correlations of H-13 (δ_H 1.11)/C-9 (δ_C 76.2), of H-12 (δ_H 1.69)/C-10 (δ_C 34.4), of H-8 (δ_H 1.51, 1.34)/C-12 (δ_C 32.7), of H-15 (δ_H 1.37)/C-6 (δ_C 74.2), C-7 (δ_C 35.5) and C-11 (δ_C 31.7), of H-10 (δ_H 3.26)/C-1 (δ_C 157.7), C-5 (δ_C 153.5), C-6 (δ_C 74.2), C-9 (δ_C 76.2) and C-10a (δ_C 109.2), and of H-1′ (δ_H 2.47 – 2.42)/C-2 (δ_C 108.4), C-3 (δ_C 143.0) and C-4 (δ_C 105.8) (Table S1; Figure S10). The planar structure of **6** was thus constructed according to the aforementioned spectroscopic data analysis. Further, the NOESY spectrum was measured in DMSO-d6 to determine the relative configuration (Figure S18). The NOESY interactions of –OH (at

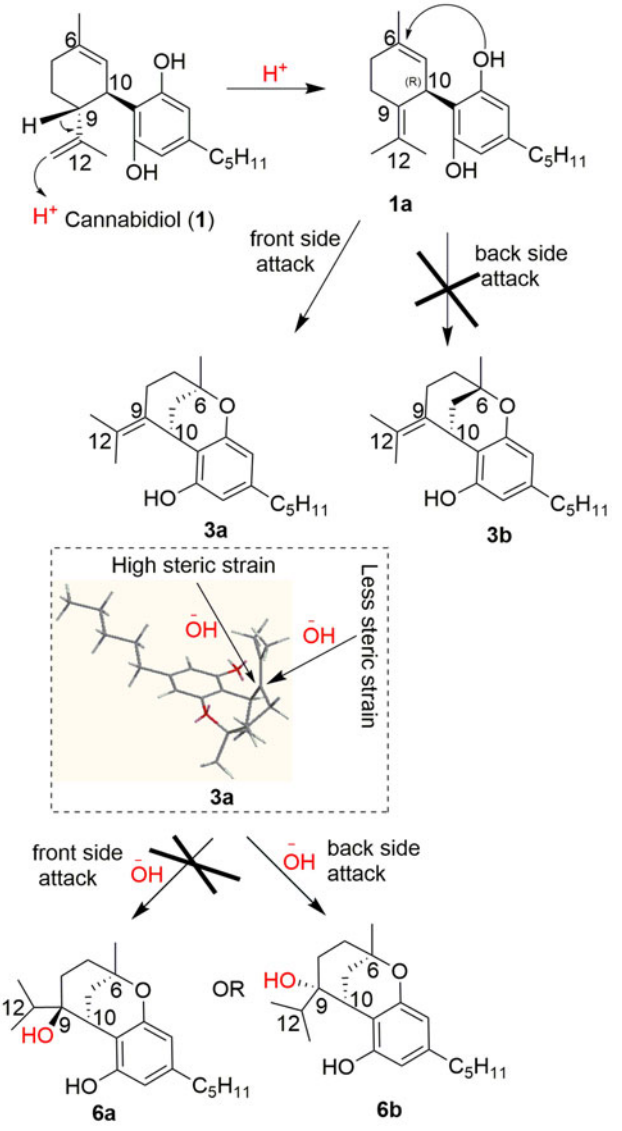

Figure 2. The plausible reaction mechanism and isomers formed in the reaction.

C-1) with H_3-13, H-12, and H-10 suggested the relative configurations at C-6, and C-10 carbons. However, the configurations of other carbons could not be assigned unambiguously because of overlapped signals in the ^{1}H NMR spectrum. To resolve the stereochemical dilemma, a plausible reaction mechanism of **6** was proposed starting from **1**. In the first step as shown in Figure 2, cannabidiol (**1**) is assumed to undergo simultaneous intramolecular cyclisation and double bond migration, thus leading to **3a** rather than **3 b** as probable intermediate. The high difference of energy ($\Delta E_{\mathbf{3a\text{-}3b}}$= -95.2 kcal/mol) computed at the accurate quantum mechanical (QM) level for both **3a** and **3 b** also clearly indicated that **3a** was the most probable intermediate in the first step. In the next step, –OH group attached at C-9 of **3a** resulting in the formation of

6a (6*R*, 9*R*, 10*S*) and **6 b** (6*R*, 9*S*, 10*S*) as possible isomers. Thereafter, ^{1}H and ^{13}C NMR chemical shifts were computed for both **6a** (6*R*, 9*R*, 10*S*) and **6 b** (6*R*, 9*S*, 10*S*) (Bifulco et al. 2007, Di Micco et al. 2010). The computed results were then compared to experimental values, allowing us to identify the configurations of **6** as those of **6 b** (6*R*,9*S*, 10*S*). Interestingly, the NOESY correlations were also found to be consistent with the **6 b** isomer. Finally, the absolute configurations were established by comparison of the experimental ECD spectrum of **6** with those predicted for **6 b** (6*R*, 9*S*, 10*S*) and for its enantiomer **6 b$_{enant}$** (6*S*, 9*R*, 10*R*) (Cerulli et al. 2017). The results showed that the calculated ECD spectrum of **6 b** was in accordance with the experimental spectrum (Figure S2). Accordingly, the absolute configuration of **6** was confidently assigned as 6*R*, 9*S*, 10*S*.

Cannabidiol (**1**) is a known cytotoxic compound against different cancer cell lines, and its mechanism of action has been thoroughly studied (Ligresti et al. 2006), especially against the breast cancer cell lines with IC_{50} values about 6 μM. Therefore, we evaluated all the compounds **(1 – 8)** for their cytotoxicity potential against a panel of eight cancer cell lines including HCT-116 (colon), MCF-7 (breast), K562 (leukemia), MIAPaCa-2 (pancreas), PANC-1 (pancreas), A549 (lung), PC-3 (prostate) and SW-620 (colon) by tetrazolium based calorimetric cytotoxicity assay (MTT assay). Cell lines were treated with different concentrations of compounds for 48 h time. Compounds **4**, **5**, **7**, and **8** showed pronounced *in vitro* cytotoxic activity against all the cell lines (Table S8) with IC_{50} values ranging from 5.6 to 60 μM. The rest of molecules **2**, **3**, and **6** were not able to induce cell death even up to 60 μM concentration (IC50 $>$ 60 μM). Out of the active molecules, compounds **4**, and **7** were found to be comparable to that of the parent molecule **1** (positive control) on the inhibition of most cancer cell lines. Taken together, our results suggest that analogs of **1** have therapeutic potential and could be further explored for their potential anticancer activity.

3. Experimental section

3.1. General experimental procedures

High-resolution mass spectra were obtained on Agilent 6540 (Q-TOF) mass spectrometer. Optical rotation was measured on a Perkin Elmer 341 polarimeter in a 1 dm cell at 25 °C. Reaction was monitored by thin layer chromatograph (TLC) on silica gel 60 F_{254} (0.25 mm thick, Merck) with spot visualized by UV 254 nm and 365 nm, and anisaldehyde reagent was used as developing agent. Column chromatography was performed using sephadex LH-20. Semi preparative HPLC was performed on an Agilent HPLC with anX Bridge Prep C8 OBD (5 μm, 1.9 × 250 mm), a photodiode array detector and auto injector function (Agilent 1260 series). ^{1}H NMR spectra were recorded (Brucker Avance) at 400 MHz and ^{13}C NMR at 100 MHz in $CDCl_3$ and DMSO-d6 chemical shifts values were reported in δ (ppm) units and coupling constants values in hertz. Tetramethylsilane (TMS) was used as internal standard. The following abbreviations were used to explain multiplicities: s = singlet, d = doublet, t = triplet, q = quartet, m = multiplet, *br* = broad. Cannabidiol (**1**) was isolated from hexane extract leaves of *Cannabis sativa* L. While other regents were purchased commercially and used without further purification, unless otherwise stated.

3.2. Procedure for preparation & isolation of compounds (2 – 8)

Cannabidiol (**1**) (1 g, 3.01 mmol) was taken in a 50 mL round bottom flask and placed in an ice bath at 0 °C containing a stirring bar. Phosphoryl chloride ($POCl_3$) (3 mL, 31.51 mmol) was added drop wise over a period of 5 min, and stirred for 5 minutes. Finally, cold saturated aqueous $NaHCO_3$ (40 mL) solution was added to quench the acid. The aqueous layer was extracted with ethyl acetate (3x100 mL), and the combined organic extracts were dried over Na_2SO_4, filtered, and concentrated in vacuo to afford a gummy viscous crude product. TLC (Hex: EtOAc 9: 1 v/v) exhibited multiple spots, which were fractionated by sephadex LH-20 column chromatography, and column was eluted with MeOH to afford four fractions (Fr.1–Fr.4), which were separated using preparative HPLC. The preparative HPLC used was equipped with Agilent 1260 series with PDA detector, X Bridge Prep C8 OBD (5 μm, 1.9 × 250 mm) column was used at a flow rate of 3.5 mL/min (column temp. 30 °C; UV detection at 215, 254 nm), and the isocratic elution was performed with 75% MeOH in water as mobile phase. Compounds **2** (135 mg, t_R 77.080 min), **3** (115 mg, t_R 79.91 min), and **4** (313 mg, t_R 82.5 min) from Fr.1 (690 mg) (Figure S20); compounds **5** (11.5 mg, t_R 40.04 min), **6** (6.1 mg, t_R 42.9 min), **7** (32 mg, t_R 50.89 min) and **8** (17 mg, t_R 58.9 min) from Fr.3 (90 mg) were isolated (Figure S21). Purified compounds were identified and characterized by HR-ESI-MS, NMR (1 D and 2 D spectroscopy) and were compared with those of the literature data.

Compound **6**: Brown, viscous oil having [α]25 *D*– 6 (*c* 1.0, acetonitrile); ^{1}H NMR ($CDCl_3$, 400 MHz) and ^{13}C NMR data, see Table S1; (+) HR-ESI-MS *m/z* 333.2421 $[M + H]^+$ (calcd for $C_{21}H_{32}O_3$ 333.2424).

3.3. Cell culture and growth conditions

A panel of Human cancer cell lines-A549 (lung), PC-3 (prostate), HCT116 (colon), MCF-7 (breast), K562 (leukemia), MIA PaCa-2 (pancreas), PANC-1 (pancreas) and SW-620 (colon) were procured from U.S. National Cancer Institute (NCI). The human cancer cell lines including A549, PC-3, T47D, HCT116, MCF-7, K562 and SW were grown in tissue culture flasks in complete growth medium (RPMI-1640) supplemented with 10% fetal bovine serum, 100 μg/mL streptomycin and 100 units/mL penicillin. MIA PaCa-2 and PANC-1 were grown in Dulbecco's minimal essential medium supplemented with 10% FBS, 2 mM L-glutamine, 3 mM sodium pyruvate, 100 units/mL penicillin, 100 μg/mL streptomycin in a carbon dioxide incubator (New Brunswick, Galaxy 170 R, Eppendorf) at 37 °C, 5% CO_2 and 98% RH.

3.4. In vitro cytotoxicity

Cell viability was determined by thiazolyl blue tetrazolium bromide (MTT) and Trypan blue assays. Briefly, 7×10^3 cells were seeded into 96-well microtitre plate and differentiated for 48 h. After differentiation and treatments with different concentrations of compounds MTT dye (2.5 mg/mL) was added and incubated for 4 h at 37 °C; after incubation, the media was aspirated and 150 μL/well DMSO was added and read at 570 nM on Mutliskan GO plate reader (Thermo Fisher Scientific, Waltham, MA, USA).

3.5. Computational details

The starting 3 D chemical structures of compounds **3a** (6 *R*, 10 *R*), **3 b** (6*S*, 10 *R*), **6a** (6 *R*, 9 *R*, 10*S*) and **6 b** (6 *R*, 9*S*, 10*S*) were built with Maestro11.1 (Schrödinger 2017). Optimizations of the starting 3 D structures were performed with Macro Model 11.5 using the OPLS force field (Jorgensen and Tirado-Rives 1988, Schrödinger 2017) and the Polak-Ribier conjugate gradient algorithm (PRCG, maximum derivative less than 0.001 kcal/mol). For these compounds, exhaustive conformational searches at the empirical molecular mechanics (MM) level with Monte Carlo Multiple Minimum (MCMM) method (50000 steps) and Low Mode Conformational Search (LMCS) method (50000 steps) were performed, in order to allow a full exploration of the conformational space. Also, molecular dynamics simulations were performed at 450, 600, 700, and 750 K, with a time step of 2.0 fs, an equilibration time of 0.1 ns, and a simulation time of 10 ns.

For each diastereoisomer, all the conformers obtained from the conformational searches were minimized (PRCG, maximum derivative less than 0.001 kcal/mol) and superimposed. Then, the "Redundant Conformer Elimination" module of Macromodel 11.5 (M. J. Frisch 2009, Schrödinger 2017) was used to select non-redundant conformers, excluding those differing more than 21.0 kJ/mol (5.02 kcal/mol) from the most energetically favoured conformation and setting a 0.5 Å RMSD (root-mean-square deviation) minimum cut-off for saving structures. All the subsequent QM calculations were performed using Gaussian 09 software (M. J. Frisch 2009, Schrödinger 2017). About compounds **3a** and **3 b**, the two most energetically favoured conformers identified at MM level were geometry optimized at the MPW1PW91/6-31G(d) level of theory. Then, the energy associated at these geometries was computed at the MPW1PW91/6-31G(d,p) level of theory and accounted for evaluating the relative stability of **3a** and **3 b**. About compounds **6a** and **6 b**, all the conformers obtained by MM conformational search rounds were optimized at the QM level using the MPW1PW91 functional and the 6-31 G(d) basis set (Cimino et al. 2004). After the optimization of the geometries, the conformers were visually inspected in order to remove further redundant conformers. The computation of the ^{13}C and ^{1}H NMR chemical shifts was performed on the selected conformers for the different diastereoisomers of compounds **6a** and **6 b**, using the MPW1PW91 functional and the 6-31 G(d,p) basis set. Final ^{13}C and ^{1}H NMR chemical shift sets of data for each of the diastereoisomers were extracted and computed considering the influence of each conformer on the total Boltzmann distribution taking into account the relative energies. Calibrations of calculated ^{13}C and ^{1}H chemical shifts were performed following the multi-standard approach (MSTD) (Tables S2–S3) (Sarotti and Pellegrinet 2009, Sarotti and Pellegrinet 2012). In particular, sp^2 ^{13}C and ^{1}H NMR chemical shifts were computed using benzene as reference compound (Sarotti and Pellegrinet 2009, Sarotti and Pellegrinet 2012), while TMS was used for computing sp^3 ^{13}C and ^{1}H chemical shift data. A further set of data was produced using only TMS as reference compound, and it was subsequently used for the computation of the DP4+ probabilities (Tables S4–S5).

Experimental and calculated ^{13}C and ^{1}H NMR chemical shifts were compared computing the $\Delta\delta$ parameter (Tables S2–S5):

$\Delta\delta = |\delta_{exp} - \delta_{calc}|$ where δ_{exp} (ppm) and δ_{calc} (ppm) were the $^{13}C/^{1}H$ experimental and calculated chemical shifts, respectively.

The mean absolute errors (MAEs) for all the considered diastereoisomers were computed using the following equation:

$$MAE = \frac{\sum(\Delta\delta)}{n}$$

defined as the summation (Σ) of the n computed absolute error values ($\Delta\delta$), normalized to the number of chemical shifts considered (n) (Tables S1–S5). Furthermore, DP4+ probabilities (Grimblat, Zanardi and Sarotti 2015) related to all the stereoisomers of **6a** and **6 b** were computed considering both ^{1}H and ^{13}C NMR chemical shifts, and comparing them with the related experimental data. In particular, since the available DP4+ Toolbox (Excel file) for the DP4+ computation allows the setting of sp^3/sp^2 atoms following the "multi-standard" approach (Sarotti and Pellegrinet 2009, Sarotti and Pellegrinet 2012), we used the chemical shift data set obtained using TMS as reference compound (Tables S4 and S5).

Concerning ECD calculations, the conformers obtained by MM experiments, as above reported, were optimized at quantum mechanical (QM) level by using the MPW1PW91 functional and the 6-31 G(d) basis set, whereas experimental solvent effects (acetonitrile) were reproduced using the integral equation formalism version of the polarizable continuum model (IEFPCM). The selected conformers were accounted for the subsequent computation of the ECD spectra of **6 b** (and of its enantiomer **6 b$_{enant}$**) (MPW1PW91//6-31G(d,p), acetonitrile IEFPCM), that were built considering the influence of each conformer on the total Boltzmann distribution and taking into account the relative energies. ECD spectrum of **6 b** (and of its enantiomer **6 b$_{enant}$**) were plotted using Spec Dis software, using a Gaussian band-shape function with the exponential half-width (σ/γ) of 0.26 eV.

Disclosure statement

No potential conflict of interest was reported by the authors.

Funding

The authors are grateful to Dr. Ram A. Vishwakarma, the Director of CSIR-IIIM Jammu for his support. We would like to acknowledge the Ministry of AYUSH (New Delhi) for providing financial support for the work of Y. K. (Z.28015/229/2015-HCP EMR), CSIR (HCP-0008) and SERB-DST (ECR/2016/000625). G. B. acknowledges the financial support of MIUR Italy PRIN 2017 project (2017A95NCJ). This manuscript represents IIIM communication number-IIIM/2291/2019. Council for Scientific and Industrial Research (CSIR), New Delhi, India; Ministry of Ayurveda, Yoga and Naturopathy, Unani, Siddha and Homoeopathy (AYUSH).

ORCID

Sajad H. Syed http://orcid.org/0000-0002-0382-4000

References

Bifulco G, Dambruoso P, Gomez-Paloma L, Riccio R. 2007. Determination of relative configuration in organic compounds by NMR spectroscopy and computational methods. Chem Rev. 107(9): 3744–3779.

Cerulli A, Lauro G, Masullo M, Cantone V, Olas B, Kontek B, Nazzaro F, Bifulco G, Piacente S. 2017. Cyclic diarylheptanoids from *Corylus avellana* green leafy covers: determination of their absolute configurations and evaluation of their antioxidant and antimicrobial activities. J Nat Prod. 80(6):1703–1713.

Cheng L-J, Xie J-H, Chen Y, Wang L-X, Zhou Q-L. 2013. Enantioselective total synthesis of (-)-Δ^8-THC and (-)-Δ^9-THC via catalytic asymmetric hydrogenation and SNAr cyclization. Org Lett. 15(4):764–767.

Cimino P, Gomez-Paloma L, Duca D, Riccio R, Bifulco G. 2004. Comparison of different theory models and basis sets in the calculation of ^{13}C NMR chemical shifts of natural products. Magn Reson Chem. 42:26–33.

Crombie L, Crombie WML, Jamieson SV, Palmer CJ. 1988. Acid catalyzed terpenylations of olivetol in the synthesis of cannabinoids. J Chem Soc, Perkin Trans 1. 1:1243–1250.

Di Marzo V, Piscitelli F. 2015. The endocannabinoid system and its modulation by phytocannabinoids. Neurotherapeutics. 12(4):692–698.

Di Micco S, Chini MG, Riccio R, Bifulco G. 2010. Quantum mechanical calculation of NMR parameters in the stereostructural determination of natural products. Eur J Org Chem. 2010(8): 1411–1434.

Grimblat N, Zanardi MM, Sarotti AM. 2015. Beyond DP4: an improved probability for the stereochemical assignment of isomeric compounds using quantum chemical calculations of NMR shifts. J Org Chem. 80(24):12526–12534.

Hanus LO, Meyer SM, Munoz E, Taglialatela-Scafati O, Appendino G. 2016. Phytocannabinoids: a unified critical inventory. Nat Prod Rep. 33(12):1357–1392.

Jorgensen WL, Tirado-Rives J. 1988. The OPLS [optimized potentials for liquid simulations] potential functions for proteins, energy minimizations for crystals of cyclic peptides and crambin. J Am Chem Soc. 110(6):1657–1666.

Ligresti A, Moriello AS, Starowicz K, Matias I, Pisanti S, De Petrocellis L, Laezza C, Portella G, Bifulco M, Di Marzo V. 2006. Antitumor activity of plant cannabinoids with emphasis on the effect of cannabidiol on human breast carcinoma. J Pharmacol Exp Ther. 318(3):1375–1387.

Luciano DP, Alessia L, Schiano MA, Marco A, Tiziana B, Stefania P, G SC, Vincenzo DM. 2011. Effects of cannabinoids and cannabinoid-enriched cannabis extracts on TRP channels and endocannabinoid metabolic enzymes. Br J Pharmacol. 163:1479–1494.

Nalli Y, Arora P, Riyaz-Ul-Hassan S, Ali A. 2018. Chemical investigation of *Cannabis sativa* leading to the discovery of a prenylspirodinone with anti-microbial potential. Tetrahedron Lett. 59(25):2470–2472.

Nalli Y, Gupta G, R.Nadkarni J, Gupta VK, Syed SH, Ali A. 2016. Divergent synthesis of prenylated carbazole alkaloid (+)-*S*-mahanimbine led to the discovery of a notch activator. RSC Adv. 6: 83069–83077.

Nalli Y, Thakur V, Mohmmed A, Kumar Gupta V, Ali A. 2017. $POCl_3$-mediated cyclization of (+)-*S*-mahanimbine led to the divergent synthesis of natural product derivatives with antiplasmodial activity. New J Chem. 41(12):4923–4930.

Radwan MM, ElSohly MA, El-Alfy AT, Ahmed SA, Slade D, Husni AS, Manly SP, Wilson L, Seale S, Cutler SJ, et al. 2015. Isolation and pharmacological evaluation of minor cannabinoids from high-potency *Cannabis sativa*. J Nat Prod. 78(6):1271–1276.

Sarotti AM, Pellegrinet SC. 2009. A Multi-standard approach for GIAO (13)C NMR calculations. J Org Chem. 74(19):7254–7260.

Sarotti AM, Pellegrinet SC. 2012. Application of the multi-standard methodology for calculating ^{1}H NMR chemical shifts. J Org Chem. 77(14):6059–6065.

Schrödinger 2017. LLC, New York NY

Seely KA, Prather PL, James LP, Moran JH. 2011. Marijuana-based drugs: innovative therapeutics or designer drugs of abuse?. Mol Interv. 11(1):36–51.

Singh AK. 2016. Exotic ancient plant introductions: part of Indian 'Ayurveda' medicinal system. Plant Genet Resour. 14(4):356–369.

Turner CE, Mole ML, Hanus L, Elsohly HN. 1981. Constituents of *Cannabis sativa*. XIX. isolation and structure elucidation of cannabiglendol, a novel cannabinoid from an Indian variant. J Nat Prod. 44(1):27–33.